



HAL
open science

A new species of *Staurosirella* (Bacillariophyta) observed in a spring of the catchment of the Regional Natural Reserve of Jolan and Gazelle Peatlands, French Massif Central, France

Aude Beauger, Elisabeth Allain, Olivier Voltaire, Christelle Blavignac,
Guillaume Caillon, Bart van De Vijver, Carlos E Wetzler

► To cite this version:

Aude Beauger, Elisabeth Allain, Olivier Voltaire, Christelle Blavignac, Guillaume Caillon, et al.. A new species of *Staurosirella* (Bacillariophyta) observed in a spring of the catchment of the Regional Natural Reserve of Jolan and Gazelle Peatlands, French Massif Central, France. *Nova Hedwigia*, 2023, 117, pp.45-59. 10.1127/nova_hedwigia/2023/0860 . hal-04292411

HAL Id: hal-04292411

<https://hal.science/hal-04292411v1>

Submitted on 17 Nov 2023

HAL is a multi-disciplinary open access archive for the deposit and dissemination of scientific research documents, whether they are published or not. The documents may come from teaching and research institutions in France or abroad, or from public or private research centers.

L'archive ouverte pluridisciplinaire **HAL**, est destinée au dépôt et à la diffusion de documents scientifiques de niveau recherche, publiés ou non, émanant des établissements d'enseignement et de recherche français ou étrangers, des laboratoires publics ou privés.



Distributed under a Creative Commons Attribution - NonCommercial - NoDerivatives 4.0
International License

1 **A new species of *Staurosirella* (Bacillariophyta) observed in a spring of the catchment of**
2 **the Regional Natural Reserve of Jolan and Gazelle Peatlands**

3
4 Aude Beauger^{1,2*}, Elisabeth Allain¹, Olivier Voldoire¹, Christelle Blavignac³, Guillaume
5 Caillon⁴, Bart Van de Vijver^{5,6} & Carlos E. Wetzel⁷

6
7 ¹Université Clermont Auvergne, CNRS, GEOLAB, F-63000 Clermont-Ferrand, France

8 ²LTSER “Zone Atelier Loire”, F-37000 Tours, France

9 ³Centre Imagerie Cellulaire Santé, UCA PARTNER, 63000 Clermont-Ferrand, France

10 ⁴Syndicat mixte du Parc naturel régional des Volcans d’Auvergne, 5 place de l’Hôtel de ville,
11 15300 Murant, France

12 ⁵Research Department, Meise Botanic Garden, Nieuwelaan 38, B-1860 Meise, Belgium

13 ⁶University of Antwerp, Department of Biology – ECOSPHERE, Universiteitsplein 1, B-2610
14 Wilrijk, Belgium

15 ⁷Luxembourg Institute of Science and Technology (LIST), Environmental Research and
16 Innovation Department (ERIN), Observatory for Climate, Environment and Biodiversity
17 (OCEB), 41 rue du Brill, 4422 Belvaux, Luxembourg

18 * *Corresponding author:* aude.beauger@uca.fr

19
20 Aude Beauger : <http://orcid.org/0000-0002-0911-0500>

21 Elisabeth Allain <http://orcid.org/0000-0002-6411-5873>

22 Olivier Voldoire <http://orcid.org/0000-0003-1306-3054>

23 Christelle Blavignac : <https://orcid.org/0000-0003-2999-7644>

24 Bart Van de Vijver: <https://orcid.org/0000-0002-6244-1886>

25 Carlos E. Wetzel: <http://orcid.org/0000-0001-5330-0494>

26 **Abstract:**

27 During a survey of headwater springs in France, an unknown *Staurosirella* taxon was
28 observed that could not be identified using the currently available literature. Based on light
29 and scanning electron microscopy observations, the taxon is described as a new species:
30 *Staurosirella luectoriana*. The new species is characterized by small isopolar, elliptical
31 frustules, connected to each other in girdle view, forming long, ribbon-like colonies via
32 bifurcating, interlocking spines. The new species presents a very small apical pore field,
33 composed of only a few pores on one valve pole. Girdle elements are variable in number,
34 closed and with an open valvocopula presenting fimbriae. *Staurosirella luectoriana* is

35 typically found in waters with high nitrate concentrations. A detailed comparison with
36 morphologically similar species is added.

37

38 **Keywords:** Europe, French Massif Central, headwaters, new species, *Staurosirella*,
39 ultrastructure

40

41 **Introduction**

42 For several years, the good ecological state of many natural ecosystems is deteriorated by
43 several negative environmental impacts such as eutrophication, linked to human impact
44 (Solimini et al. 2006). Moreover, natural environments are also affected by climate change as
45 it represents one of the principal threats for freshwater biodiversity (Dudgeon et al. 2006;
46 Woodward et al. 2010). Peatbog ecosystems, and the headwaters feeding them, are strongly
47 impacted by these effects, resulting in physical and chemical alterations, such as an increase
48 in surface water temperature and, most likely, a possible increase of hydrological drought
49 duration (Kaule & Frei 2022). These abiotic modifications influence the species composition
50 and dynamics of biological communities. Anthropogenic pressures, such as agricultural uses
51 exerted on these fragile ecosystems and their watersheds, can also contribute to degrading
52 their quality and altering their biodiversity, further threatening the conservation of their good
53 condition and compromising the ecosystem services provided by these environments (Bernard
54 2016).

55 When considering the watershed, springs giving rise to streams flowing through peatland, are
56 classified as unique aquatic habitats, contributing significantly to local and regional
57 biodiversity due to their high habitat complexity” (Cantonati et al. 2012). Springs usually are
58 species-rich habitats and it is well known that abiotic factors such as water chemistry and
59 temperature are important ecological factors determining species distribution and community
60 composition. They also are widely threatened by both regional and global factors, including
61 pollution and climate change leading to changes in biodiversity and species composition
62 (Stevens et al. 2021). As biodiversity is the keystone of the functioning of these ecosystems
63 from which ecosystem services are derived, it is important to protect the water catchment and
64 to increase our knowledge of it.

65 The Regional Nature Reserve (RNR) of the Jolan and Gazelle peatlands, situated in the
66 French Massif Central, was created in 2018 for the protection of the peatlands inhabiting
67 numerous plant and animal species (including several rare) such as the endangered dragonfly
68 *Somatochlora arctica* Zetterstedt. The area is highly impacted by the eutrophication of the
69 minerotrophic peatlands adjoining the Jolan pond urging for a detailed (impact) study of the
70 Nature Reserve. One of the aspects already studied included the diatom flora together with a
71 physical and chemical analysis of the pond. The study was carried out in the reserve
72 (peatlands and watershed) in June 2022. During this survey, a small-celled species belonging
73 to the genus *Staurosirella* was observed in one of the springs of the watershed that could not
74 be identified using the currently available literature on the genus.

75 The genus *Staurosirella* D.M.Williams & Round (1987: 274) was originally described in
76 1987, and further emended in 2006 by Morales & Manoylov. This genus comprises small-
77 celled araphid species showing an oval, elliptical, cruciform, occasionally triangular valve
78 outline (Round et al. 1990). The genus is further characterized by the presence of well-
79 developed marginal spines such as in *S. lapponica* (Grunow) D.M.Williams & Round,
80 allowing the formatting of long chain-like colonies, incipient such as in *S. berolinensis*
81 (Lemmerm.) Bukht. (Bukhtiyarova 1995) or absent as is the case in several species such as *S.*
82 *lanceolata* (Hust.) E. Morales et al. (Morales et al. 2010). *Staurosirella* species possess
83 uniseriate striae typically composed of areolae that can be circular or elliptical, occasionally
84 transapically elongated, internally occluded by volae (Williams & Round 1987; Round et al.
85 1990; Morales & Manoylov 2006; Morales et al. 2019a). Apical pore fields are quite variable
86 in size and shape but are always composed of several rows of round areolae disposed in
87 ordered rows (Morales & Manoylov 2006). Finally, the cingulum is composed of several
88 plain, open or closed copulae lacking ligulae (Morales & Manoylov 2006; Van de Vijver et al.
89 2022), with the valvocopula being considerably larger and possessing fimbriae attached to the
90 costae at the valve interior (Morales & Manoylov 2006; Van de Vijver 2022). *Staurosirella*
91 species occur worldwide in a wide variety of freshwater habitats such as rivers, reservoirs,
92 lakes and pools (Almeida et al. 2015; Guerrero et al. 2019; Morales & Edlund 2003; Morales
93 et al. 2010; Seeligmann et al. 2018; Van de Vijver et al. 2014). Currently, AlgaeBase (Guiry
94 & Guiry 2022) lists almost 60 names are listed under *Staurosirella* (including 53 species and
95 5 varieties).

96 Following detailed light microscopy (LM) and scanning electron microscopy (SEM)
97 observations and comparisons with known representatives of this genus, the small-celled
98 *Staurosirella* found in the Jolan and Gazelle peatlands RNR is described as a new species:
99 *Staurosirella luectoriana* Beauger, C.E.Wetzel & Van de Vijver, sp. nov. The morphology
100 of the new species is compared with the most similar *Staurosirella* taxa occurring worldwide.
101 Notes on its ecological preferences are added.

102

103 **Materials and Methods**

104 The Jolan and Gazelle peatlands RNR is located at the head of the Adour-Garonne watershed
105 (Rhue catchment) near the city of Ségur-les-Villas (Cantal, Auvergne, France) (Fig. 1). The
106 RNR, located at 1,130 m a.s.l. on the volcanic plateau of Cézallier, is part of the French
107 Massif Central and influenced by oceanic, continental, and Mediterranean climate. The total
108 area of 155 ha is essentially occupied by habitats of regional or even national interest. This

109 protected area shelters peat bogs of major interest for the Auvergne region and the massif.
110 Part of the meadows and grasses in the watershed of these wetlands are also included in the
111 protection perimeter. The studied spring, situated in pastures, is located at 1,143 m a.s.l., and
112 emerges in a concrete drinking trough (Fig. 1d).

113 On the 15th June 2022, an epilithic sample was taken using a toothbrush, brushing, the
114 drinking trough. Sample was preserved with an ethanol solution to a final concentration of
115 70%. *In-situ*, pH, conductivity ($\mu\text{S cm}^{-1}$) and water temperature ($^{\circ}\text{C}$) were measured using a
116 WTW Multiline P4. For dissolved oxygen (% saturation and mg L^{-1}), a ProODO oxygen
117 probe was used. Two water samples were collected for further chemical analysis in the
118 laboratory and were analysed using high pressure ion chromatography methods. On one
119 sample, carbonate concentration (HCO_3^-) (mg L^{-1}) was measured using a HACH Digital
120 Titrator, sulfuric acid (0.1600 N and 1.600 N) and the Bromocresol Green-Methyl Red
121 Indicator (Hach method 8203). The second sample was filtered using Whatmann GF/C filters
122 prior to analysis. A Thermo Scientific Dionex ICS1100 system was used for the cation
123 analysis and, for the anions, the Thermo Scientific Dionex Aquion system was applied. The
124 concentrations of lithium, sodium, ammonium, potassium, magnesium, calcium, fluoride,
125 chloride, nitrite, nitrate, phosphate and sulphate were measured (mg L^{-1}) (Table 1).

126 Samples were prepared for LM and SEM observations following the method described in
127 Prygiel & Coste (2000) cleaning a small sub-sample of epilithic raw material with hydrogen
128 peroxide (H_2O_2 , 35% v/v;) and hydrochloric acid (HCl 37% v/v). The sample was then rinsed
129 several times and subsequently diluted with distilled water to avoid excessive concentrations
130 of diatom valves on the slides. Finally, a drop of the diluted cleaned material was dried on
131 coverslips and mounted in Naphrax[®]. LM observations and morphometric measurements
132 were performed using a Leica[®] DM2700M at 1000X magnification (N.A. 1.30), equipped
133 with Differential Interference Contrast (Nomarski) optics. Light micrographs were taken with
134 a Leica[®] DMC2900 camera. At least 400 diatom valves were enumerated on random
135 transects to get an overview of the composing diatom flora, and converted into percentage
136 relative abundance.

137 For SEM, parts of the oxidized suspensions were and inore filtered with additional deionized
138 water through a 0.2 μm Isopore polycarbonate membrane filter. Pieces of which were fixed on
139 aluminum stubs after air-drying and coated with a 2 nm layer of chrome, using a high vacuum
140 coating with a 5nm Chrome layer using 100mA (1 minute) in a Quorum sputter coater (Q150
141 TES Plus). Then, it was studied using a Hitachi Regulus 8230 ultrahigh-resolution analytical

142 field emission (FE) scanning electron microscope (Hitachi High-Technologies Corporation,
143 Japan), operated at 2 kV and 10 mm working distance.
144 Plates were prepared using Adobe InDesign 16.4. Samples and slides are stored at the
145 Herbiers Universitaires de Clermont-Ferrand (CLF) (France) and Meise Botanic Garden (BR)
146 (Belgium). Diatom terminology follows Ross et al. (1979), Barber & Haworth (1981) for
147 terminology related to valve shape and striae orientation (valve shape, stria/areola structure)
148 and Round et al. (1990) for terminology on areolar substructures and girdle band features.
149 Taxonomic comparisons referred to the following publications: Guerrero et al. (2019),
150 Morales et al. (2015; 2019b), Osório et al. (2021) and Van de Vijver et al. (2022).

151

152 **Results**

153 Division Bacillariophyta

154 Class Bacillariophyceae

155 Subclass Fragilariophycidae

156 Order Fragilariales

157 Family Staurosiraceae

158 Genus *Staurosirella* D.M. Williams & Round 1987

159 ***Staurosirella luectoriana* Beauger, C.E. Wetzel & Van de Vijver sp. nov.**

160 PhycoBank registration: <http://phycobank.org/103828>

161 **Light microscopy** (Figs 2–37): frustules rectangular in girdle view (Fig. 35), connected to
162 each other to form long, ribbon-like colonies (Figs 36–37). Valves isopolar, elliptical; longer
163 valves with weakly parallel margins and shorter valves with convex margins. Apices broadly
164 rounded. Valves dimensions (n=45): length 5.5–8.5, width 3–4.5. Very little size variation
165 observed. Sternum narrow. Central area absent. Striae equidistant, running continuously from
166 apex to apex, broad, 10–12 in 10 µm. Striae parallel in the middle becoming radiate near the
167 apices. Areolae not discernible in LM.

168 **Scanning electron microscopy** (Figs 38–47): Frustules linked by marginal bifurcating and
169 interlocking spines (Figs 38–39). Spines, originating from a single point, well-developed, and
170 dichotomously branched, with a circular columnar base (Figs 39–40), located on the virgae
171 between the striae at the valve face/mantle junction (Figs 40–41). Valve face externally
172 uneven with raised virgae and sternum and adjacent striae slightly sunken in ‘punch hole-like’
173 depressions. Striae uniseriate, composed of long, slit-like, linear areolae, running almost
174 parallel to the apical axis (Figs 40–41) or with two terminal striae located on top of the
175 continuation of the axial area onto the mantle (Fig. 42), with areolae in size gradually

176 narrowing at both ends (Figs 40, 44–45). Volae projected towards the valve interior (Fig. 41).
177 Externally, volae intertwining at the same level as their points of origin (Fig. 41). Vimines
178 long and narrow becoming longer toward the valve face edge (Fig. 41). Sternum narrowly
179 lanceolate (Figs 40–41, 44). Mantle rather deep (Fig. 44) with small siliceous plaques located
180 at the mantle edge (Fig. 39, arrow). Apical pore field (APF) present on one apex, occasionally
181 absent, located on the valve face/mantle junction, very small, composed of only one pore or a
182 possibly reduced lineola (Figs 41, 45, arrows). On the other apex, apical pore field replaced
183 by vestiges of a stria (Fig. 44). Internally, striae clearly sunken between flattened virgae and
184 sternum (Figs 42–43). Girdle elements variable in number, closed (Figs 38, 46–47). Open
185 alvocopula showing reduced fimbriae (Fig. 46).

186

187 **Holotype:** CLF121600 (Herbiers Universitaires de Clermont-Ferrand, France)

188 **Isotype:** BR-4802 (Meise Botanic Garden, Belgium)

189 **Type locality:** FRANCE, spring of the Regional Nature Reserve of the Jolan and Gazelle
190 peatlands at Ségur-les-Villas, E688741.423 and N6455250.009 (Lambert 93)

191 **Etymology:** The new species is named in honour to our friend Luc Ector (1962–2022).

192 **Ecology:** The well-oxygenated spring was characterized by low conductivity and slightly
193 acidic waters (Table 2). The concentration in nitrates was high with 22 mg L⁻¹.

194 The diatom flora in the spring was dominated by *S. lucectoriana* (44% of all counted
195 diatoms), *Nitzschia fonticola* (Grunow) Grunow (28%) and *N. soratensis* E.Morales & Vis
196 (7.5%). Other, less frequent (<5%) taxa include *Amphora indistincta* Levkov (3.7%),
197 *Navicula veneta* Kütz. (3%), *Staurosira* cf. *sviridae* Kulikovskiy et al. (3%), *Sellaphora*
198 *atomoides* C.E.Wetzel & Van de Vijver (2%), *Encyonema minutum* (Hilse) D.G.Mann
199 (1.5%), *Planothidium lanceolatum* (Bréb. ex Kütz.) Lange-Bert. (1.4%), *Nitzschia linearis*
200 (C.Agardh) W.Sm. (1.1%). At last, *Achnantheidium eutrophilum* (Lange-Bert.) Lange-Bert.,
201 *Adlafia minuscula* (Grunow) Lange-Bert., *Amphora copulata* (Kütz.) Schoeman &
202 R.E.M.Archibald, *Cocconeis rouxii* Hérib. & Brun, *Diatoma mesodon* (Ehrenb.) Kütz.,
203 *Encyonema ventricosum* (Kütz.) Grunow, *Meridion circulare* (Grev.) C.Agardh, *Navicula*
204 *cryptocephala* Kütz., *Navicula gregaria* Donkin, *Nitzschia alpina* Hust., *Nitzschia palea* var.
205 *tenuirostris* Grunow, *Planothidium curtistriatum* C.E.Wetzel et al., *Planothidium*
206 *frequentissimum* (Lange-Bert.) Lange-Bert., *Psammothidium lauenburgianum* (Hust.)
207 Bukhtiyarova & Round and *Sellaphora crassulexigua* (E.Reichardt) C.E.Wetzel & Ector
208 represented each one less than 1% of the whole community.

209

210 **Discussion**

211 *Staurosirella lucectoriana* is one of the few *Staurosirella* species known to form long, chain-
212 like colonies. At present, only two other *Staurosirella* species form similar colonies: *S.*
213 *lapponica* (Grunow) D.M.Williams & Round and *S. mutabilis* (W.Sm.) E.Morales & Van de
214 Vijver. These three species share some morphological features such as the typical
215 interlocking, bifurcating spines that can also be seen in for instance *S. lapponica* (Van de
216 Vijver et al. 2022), and the reduced apical pore fields. Both *S. lapponica* and *S. mutabilis*,
217 however, possess a very broad sternum, compared to *Staurosirella lucectoriana*, formed by
218 reduced marginal striae (Morales et al. 2015; Van de Vijver et al. 2022). Contrary, *S.*
219 *lucectoriana* presents striae that almost reach each other on the sternum.

220 It appears that the type population observed of *Staurosirella lucectoriana* present very little
221 size variation. Thus, based on valve outline and morphometric dimensions, only three
222 *Staurosirella* species show some resemblance, although they all lack the typical colony
223 formation and bifurcating spines (Table 2): *S. andinopatagonica* J.M.Guerrero et al., *S.*
224 *neopinnata* E.Morales et al. and *S. paranaensis* N.C.Osório et al. (Guerrero et al. 2019;
225 Morales et al. 2019b; Osório et al. 2021). *Staurosirella neopinnata* often has longer, more
226 elongated valves with almost parallel margins, a pattern not observed in *S. lucectoriana*,
227 where only rounded to elliptical valves were observed with convex margins. In outer view,
228 the striae in *S. paranaensis* are narrower due to more heavily build, clearly raised virgae,
229 contrary to *S. lucectoriana* that possesses striae almost equal in width as the virgae (Osório et
230 al. 2021, see for instance figs 35 & 38). *Staurosirella andino-patagonica* has two thin spines
231 per virga, and lacks the robust bifurcating spines of *S. lucectoriana* (Guerrero et al. 2019).
232 Moreover, *S. andino-patagonica* has less raised external virgae with the striae therefore less
233 sunken between them.

234 The reduced apical pore field, observed in *S. lucectoriana*, is typical for colony-forming
235 *Staurosirella* species and was also encountered in *S. lapponica* and *S. mutabilis* (Morales et
236 al. 2015, see fig. 45; Van de Vijver et al. 2022, see fig. 30). The ability to form colonies by
237 linking spines reduced the need to connect cells via the apices and therefore larger apical pore
238 fields seem less necessary. Apart from the colony-forming species, several solitary
239 *Staurosirella* species also have reduced apical pore fields, such as *S. andinopatagonica*, *S.*
240 *krammeri* E.Morales et al., *S. neopinnata* and *S. paranaensis*, that all have an apical pore field
241 composed of only a few small pores. This is in clear contrast with other *Staurosirella* species
242 showing large pore fields with long, regular rows of small pores such as *S. baicalensis* with an
243 APF widely extended on the foot poles and less on the head poles (Kulikovskiy et al. 2015), *S.*

244 *dubia* (Grunow) E.Morales & Manoylov (Morales & Manoylov 2006) and *S. minuta*
245 E.Morales & Edlund (Morales & Edlund 2003) with APF composed of several discernible
246 rows of round poroids at both apices. Morales et al. (2010) discussed several small-celled
247 *Staurosirella* species that, despite their reduced valve dimensions, still possess well-
248 developed apical porefields, making the APF of the new species rather unique.
249 Compared to other small round-celled species, the valvocopula of the new species is also
250 closed and the other girdle bands are closed.
251 Considering the internal view, it appears that no feature differs between the species except
252 that for *S. andinopatagonica*, areolae are occluded by delicate and dichotomously branched
253 volae while for the other including the new species, volae are projected towards the valve
254 interior. At last, for all species, the striae are in depressions.
255 When considering the ecology of the new species, *Staurosirella luectoriana* was observed in
256 a headwater spring that emerges in a concrete drinking trough. The high nitrate concentration
257 reflected the impact of agricultural activities in the catchment (Taboada-Castro et al. 2004).
258 The new species was associated with two freshwater species: *Nitzschia fonticola*, known to
259 live in oligo- to beta-mesosaprobic and meso-eutrophic environments and *Nitzschia*
260 *soratensis*, preferring slightly eutrophic to eutrophic waters pointing out the presence of
261 nutrients in the spring (Van Dam et al. 1994; [Lange-Bertalot et al. 2017](#)).
262 When considering the other species compared to the new one, they were encountered in
263 different environments: *S. andinopatagonica* and *S. neopinnata* were described in lake
264 samples and sediment core and, *S. paranaensis* was first observed in a large river.
265 *Staurosirella mutabilis* was observed in fresh water but there was no information on the
266 physical and chemical parameters of the habitat. Likewise, for *S. lapponica*, information on
267 the ecological characteristics of its type habitat is lacking.
268 This study underlined the presence of a particular diatom biodiversity in the RNR of the Jolan
269 and Gazelle peatlands, with the presence of new species and others are under review. This
270 confirms the interest to have created a reserve in this area and the necessary to protect it and
271 to continue care. It will be interested to to increase our knowledge on the diatom biodiversity
272 and to do other surveys done in other mountainous areas of the French Massif Central.

273

274 **Acknowledgements**

275 Funding for this research was partly provided by funded by the Direction Régionale de
276 l'Environnement, de l'Aménagement et du Logement Auvergne-Rhône-Alpes, and by the

277 “Réserve naturelle régionale des tourbières du Jolan et de la Gazelle” and in the framework of
278 the DIATOMS project (LIST-Luxembourg Institute of Science and Technology).

279 Anonymous reviewers are thanked for their valuable comments.

280

281 **References**

282 Almeida, P.D., Wetzel, C.E., Morales, E.A., Ector, L. & Bicudo, D.C. (2015). *Staurosirella*
283 *acidophila* sp. nov., a new araphid diatom (Bacillariophyta) from southeastern Brazil:
284 ultrastructure, distribution and autecology. *Cryptogam. Algologie* 36(3), 255–270.

285 <https://doi.org/10.7872/crya/v36.iss3.2015.255>

286 Barber, H.G. & Haworth E.Y. (1981). A guide to the morphology of the diatom frustule with
287 a key to the British freshwater genera. *Sci. Publ. Freshwater Biol. Assoc.* 44, 1–112.

288 Bernard, G. (2016). Panorama des services écosystémiques des tourbières en France. Quels
289 enjeux pour la préservation et la restauration de ces milieux naturels ? Pôle-relais Tourbières.
290 Fédération des Conservatoires d’espaces naturels, 47p.

291 Bukhtiyarova, L.N. (1995). Novye taksonomicheskie kombinatsii diatomovykh vodoroslei
292 (Bacillariophyta). [New taxonomic combinations of diatoms (Bacillariophyta)]. *Algologia*
293 5(4), 417–424.

294 Cantonati, M., Füreder, L., Gerecke, R., Jüttner, I. & Cox, E.J. (2012). Crenic habitats,
295 hotspots for freshwater biodiversity conservation: toward an understanding of their ecology.
296 *Freshw. Sci.* 31(2), 463–480. <https://doi.org/10.1899/11-111.1>

297 Dudgeon D., Arthington, A., Gessner, M., Kawabata, Z.-I., Knowler, D., Lévêque, C.,
298 Naiman, R., Prieur-Richard, A.-H., Soto D., Stiassny M. & Sullivan, C. (2006). Freshwater
299 biodiversity: importance, threats, status and conservation challenges. *Biol Rev Camb Philos*
300 *Soc* 81, 163–182. <https://doi.org/10.1017/S1464793105006950>

301 Guerrero, J.M., Luján García, M. & Morales, E.A. (2019). *Staurosirella andinopatagonica* sp.
302 nov. (Bacillariophyta) from lake sediments in Patagonia, Argentina. *Phytotaxa* 402(3) 131–
303 144. <https://doi.org/10.11646/phytotaxa.402.3.1>

304 Guiry, M.D. & Guiry, G.M. (2022). AlgaeBase. World-wide electronic publication, National
305 University of Ireland, Galway. Available from: <http://www.algaebase.org> (accessed 11
306 January 2023).

307 Kaule, L. & Frei, S. (2022). Analysis of drought conditions and their impacts in a headwater
308 stream in the Central European lower mountain ranges. *Reg. Environ. Change* 22, 82.

309 <https://doi.org/10.1007/s10113-022-01926-y>

310 [Kulikovskiy, M.S., Lange-Bertalot, H. & Kuznetsova, I.V. \(2015\). Lake Baikal: hotspot of](#)
311 [endemic diatoms II. *Iconogr. Diatomol.* 26, 1–656.](#)

312 [Lange-Bertalot, H., Hofmann, G., Werum, M., Cantonati, M. \(2017\). *Freshwater Benthic*](#)
313 [Diatoms of Central Europe: Over 800 Common Species Used in Ecological Assessment;](#)
314 [English Edition with Updated Taxonomy and Added Species. Cantonati, M., Kelly, M.G.,](#)
315 [Lange-Bertalot, H., Eds.. Koeltz Botanical Books: Schmittgen-Oberreifenberg.](#)
316 *the genera*. Cambridge: Cambridge University Press.

317 Morales, E.A., Wetzel, C.E., Novais, M.H., Buczkó, K, Morais, M.M. & Ector, L. (2019a).
318 Morphological reconsideration of the araphid genus *Pseudostaurosira* (Bacillariophyceae), a
319 revision of *Gedaniella*, *Popovskayella* and *Serratifera*, and a description of a new
320 *Nanofrustulum* species. *Plant Ecol Evol.* 152(2), 262–284.
321 <https://doi.org/10.5091/plecevo.2019.1604>

322 Morales, E.A., Wetzel, C.E., Haworth, E.Y. & Ector, L. (2019b). Ending a 175-year
323 taxonomic uncertainty: Description of *Staurosirella neopinnata* sp. nov. (Bacillariophyta) to
324 accommodate *Fragilaria pinnata*, a highly misconstrued taxon with a purported worldwide
325 distribution. *Phytotaxa* 402(2), 75–87.

326 Morales, E.A, Wetzel, C.E, Van de Vijver, B. & Ector, L. (2015). Morphological studies on
327 type material of widely cited araphid diatoms (Bacillariophyta). *Phycologia* 54(5), 455–470.
328 <https://doi.org/10.2216/15-21.1>

329 Morales, E.A., Wetzel, C.E. & Ector, L. (2010). Two short striated species of *Staurosirella*
330 (Bacillariophyceae) from Indonesia and the United States. *Pol. Bot. J.* 55(1), 107–117.

331 Morales, E.A. & Manoylov, K.M. (2006). *Staurosirella incognita* Morales et Manoylov sp.
332 nov., a non-spiny species from North America, with an emended description of *Staurosirella*
333 Williams et Round (Bacillariophyceae). In: Witkowski A. (ed.) *Proceedings of the Eighteenth*
334 *International Diatom Symposium* (pp. 25–336). Międzyzdroje, Poland.

335 Morales, E. & Manoylov, K.M. (2006). Morphological studies on selected taxa in the genus
336 *Staurosirella* Williams et Round (Bacillariophyceae) from rivers in North America. *Diatom*
337 *Res.* 21(2): 343–364.
338 <https://doi.org/10.1080/0269249X.2006.9705674>

339 Morales, E.A. & Edlund, M.B. (2003). Studies in selected fragilarioid diatoms
340 (Bacillariophyceae) from Lake Hovsgol, Mongolia. *Phycol. Res.* 51(4): 225–239.
341 <https://doi.org/10.1111/j.1440-1835.2003..x>

342 Osório, N.C., Ector, L., Rodrigues, L., & Wetzel, C.E. (2021). *Staurosirella paranaensis* sp.
343 nov., a new epiphytic freshwater diatom (Bacillariophyceae) from the Paraná River

344 floodplain, Brazil, South America. *Phytotaxa* 480(2), 163–173.
345 <https://doi.org/10.11646/phytotaxa.480.2.5>

346 Prygiel, J. & Coste (2000) M. *Guide méthodologique pour la mise en oeuvre de l'indice*
347 *Biologique Diatomées* NF T 90-354. Agences de l'Eau, Cemagref de Bordeaux, Bordeaux.

348 Ross, R., Cox, E.J., Karayeva, N.I., Mann, D.G., Paddock, T.B.B., Simonsen, R & Sims, P.A.
349 (1979). An emended terminology for the siliceous components of the diatom cell. *Nova*
350 *Hedwigia Beih.* 64, 513–533.

351 Round, F.E., Crawford, R.M. & Mann, D.G. (1990). *The diatoms biology and morphology of*
352 *the genera*. Cambridge: Cambridge University Press.

353 Seeligmann, C.T., Maidana, N.I. & Morales, E.A. (2018). Fragilariaceae (Bacillariophyta) en
354 humedales de altura de Catamarca (Argentina). *Bol. Soc. Argent. Bot.* 53(4): 507–519.
355 <https://doi.org/10.31055/1851.2372.v53.n4.21975>

356 Solimini, A., Cardoso, A.C. & Heiskanen, A.-S. (eds) (2006). Indicators and methods for the
357 Ecological Status Assessment under the Water Framework Directive. Linkages between
358 chemical and biological quality of surface waters. EUR 22314 EN. European Commission.

359 Stevens, L.E., Schenk E.R. & Springer A.E. (2021). Springs ecosystem classification. *Ecol*
360 *Appl.* 31, e2218. <https://doi.org/10.1002/eap.2218>.

361 Taboada-Castro, M.M., Diéguez-Villar, A. & Taboada-Castro, M.T. (2004). Transfer of
362 nutrients and major ions of an agricultural catchment to runoff waters: analysis of their spatial
363 distribution. 13th International Soil Conservation Organisation Conference, Brisbane.

364 Van de Vijver, B., Morales, E.A., Schuster, T.M., Wetzel, C.E., & Ector, L. (2022).
365 Typification and morphology of *Staurosirella lapponica* (Grunow) D.M. Williams & Round
366 and *Staurosirella pinnata* var. *intercedens* (Grunow) P.B. Hamilton (Staurosiraceae,
367 Bacillariophyta). *Nova Hedwigia*, 115(1–2), 31–45.
368 https://doi.org/10.1127/nova_hedwigia/2022/0697

369 Van de Vijver, B. 2022. Two new *Staurosirella* species (Staurosiraceae, Bacillariophyta)
370 observed in an historic Rabenhorst sample. *Phytotaxa* 545(2), 163–174.
371 <https://doi.org/10.11646/phytotaxa.545.2.5>

372 Van de Vijver, B., Morales, E.A. & Kopalová, K. (2014). Three new araphid diatoms
373 (Bacillariophyta) from the Maritime Antarctic Region. *Phytotaxa* 167(3), 256–266.
374 <https://doi.org/10.11646/phytotaxa.167.3.4>

375 Van Dam, H., Mertens, A., Sinkeldam, J.A (1994). coded checklist and ecological indicator
376 values of freshwater diatoms from The Netherlands. *Neth. J. Aquat. Ecol.* 28, 117–133.
377 <https://doi.org/10.1007/BF02334251>

378 Williams, D.M. & Round, F.E. (1988 '1987'). Revision of the genus *Fragilaria*. *Diatom Res.*
379 2, 267–288. <https://doi.org/10.1080/0269249X.1987.9705004>
380 Woodward, G., Perkins, D.M. & Brown, L.E. (2010). Climate change and freshwater
381 ecosystems: impacts across multiple levels of organization. *Philos Trans R Soc Lond B Biol*
382 *Sci* 365, 2093–2106. <https://doi.org/10.1098/rstb.2010.0055>
383
384

385 **Figure legends**

386 Figure 1. Map showing the location of the study spring. a and b: general location of the spring
387 in France and in the Auvergne region; c: location of the spring (blue circle) in Regional
388 Nature Reserve (RNR) of the Jolan and Gazelle peatlands; d: photography of the studied
389 spring.

390 Figures 2–43. *Staurosirella lucectoriana* sp. nov. Figs 2–37. LM. Type population of a spring
391 of the RNR of the Jolan and Gazelle peatlands, France. Scale bar = 10 μm . Figs 38–43. SEM.
392 Figs 38. External view of two frustules and one valve connected to each other with
393 dichotomously branched and interlocking spines. Fig. 39. External detail of the linking spines.
394 The arrow indicates the presence of mantle plaques. Fig. 40. External view of an entire valve.
395 Fig. 41. External detail of the apex. The arrow indicates the reduced APF. Fig. 42. Internal
396 view of an entire valve. Fig. 43. Internal detail of the apex. Scale bar = 5 μm (Fig. 38), 4 μm
397 (Figs 40, 42), 3 μm (Fig. 39) and 1 μm (Figs 41, 43).

398 Figures 44–47. Fig 44. External view of a tilted valve. Apical pore field replaced by vestiges
399 of a stria, reduced to rounded areolae. Fig. 45. External view of the apex. The arrow indicates
400 the reduced APF composed of only one pore. The isolated pore subtends an apical spine and
401 always seem to be off the apical axis. Figs 46–47. Valvocopula bearing fimbriae. Scale bar =
402 5 μm (Fig. 44), 4 μm (Figs 46, 47) and 2 μm (Fig. 45).

403

404

405

406

407

408

409

410

411

412

413

414

415

416

417

418

419 Table 1: Physical variables and chemical variables measured in the spring.

Date	15/06/2022
Conductivity ($\mu\text{S cm}^{-1}$)	127.5
pH (pH units)	6.46
Temperature ($^{\circ}\text{C}$)	12.4
Dissolved oxygen (%)	93.4
Li^+ (mg L^{-1})	<0.005
Na^+ (mg L^{-1})	5.20
NH_4^+ (mg L^{-1})	<0.005
K^+ (mg L^{-1})	2.72
Mg^{2+} (mg L^{-1})	5.01
Ca^{2+} (mg L^{-1})	9.89
F^- (mg L^{-1})	0.05
Cl^- (mg L^{-1})	6.83
NO_2^- (mg L^{-1})	0.01
NO_3^- (mg L^{-1})	22.05
PO_4^{3-} (mg L^{-1})	0.05
HCO_3^- (mg L^{-1})	35.8
SO_4^{2-} (mg L^{-1})	1.89

420

421

422 Table 2: Main characteristics of *Staurosirella luectoriana* and 5 similar *Staurosirella* species.

	Reference	Valve length (µm)	Valve width (µm)	Number of striae (in 10µm)	Valve outline	Striae	Spines	Axial area	Apical pore fields	V
<i>Staurosirella luectoriana</i>	This study	5.5–8.5	3.0–4.5	10.0–12.0	Isopolar, elliptical; longer valves with weakly parallel margins and shorter valves with convex margins	Uniseriate, composed of long, slit-like, linear areolae, running parallel to the apical axis, with areolae in size gradually narrowing at both ends	Originating from a single point, well-developed, dichotomously branched, with a circular columnar base, located on the virgae between the striae at the valve face/mantle junction	Narrowly lanceolate	Present on at least one apex, located on the valve face/mantle junction, very small, composed of only one pore. On the other apex, APF replaced by vestiges of a stria, reduced to rounded areolae	C
<i>Staurosirella andinopatagonica</i>	Guerrero et al. (2019)	4.4–6.5	2.4–3.7	(8)11.0–13.0(15)	Isopolar to slightly heteropolar, broadly elliptic	Uniseriate, uninterrupted from valve face to valve mantle	2 spines, exceptionally 1 or 3, located on virgae, conical	Narrow, linear to slightly lanceolate	More developed at one pole, composed of 2–3	C p

						and composed of slit-like areolae oriented parallel to the apical axis	and parallel, anastomosing at the base		rows of small, round poroids	
<i>Stausosirella lapponica</i>	Van de Vijver et al. (2022)	7.0–35.0(40)	4.0–6.0	6.0–7.0	Linear to linear-elliptic, isopolar	Short, extending to about 1/3 of the valve mantle	Present, hollow, circular base, upper portion a thick V-shaped with bifurcate lateral extensions	Wide	Reduced on both poles	N
<i>Stausosirella mutabilis</i>	Morales et al. (2015)	8.5–26.0	4.0–25.0	8.0–9.0	Elliptic, isopolar	Short, extending to mid valve mantle	Present, hollow, elliptic base, upper portion diapason shape with pointy lateral extensions.	Wide	Reduced on both poles	C
<i>Stausosirella neopinnata</i>	Morales et al. (2019b)	4.0–25.0	4.0–4.7	8.0–9.5	Elliptical, most frequently isopolar to rarely slightly heteropolar	Uninterrupted from valve face to mantle	Originating from two (rarely three) points on each virgae at the valve face-mantle	Narrowly lanceolate	Reduced or developed, equal size at both poles	C

							junction, initially hollow, tip spatulate		
<i>Stausosirella paranaensis</i>	Osório et al. (2021)	6.0–10.0	3.0–4.5	8.0–11.0	Elliptical, most frequently isopolar to rarely slightly heteropolar	Uninterrupted from valve face to mantle	Solid and thin; one per costa, originating from one point on each virgae at the valve face-mantle junction, initially hollow, tip spatulate	Narrowly lanceolate	Usually equally developed on both valve poles composed of round poroids

423

424

425

426

427

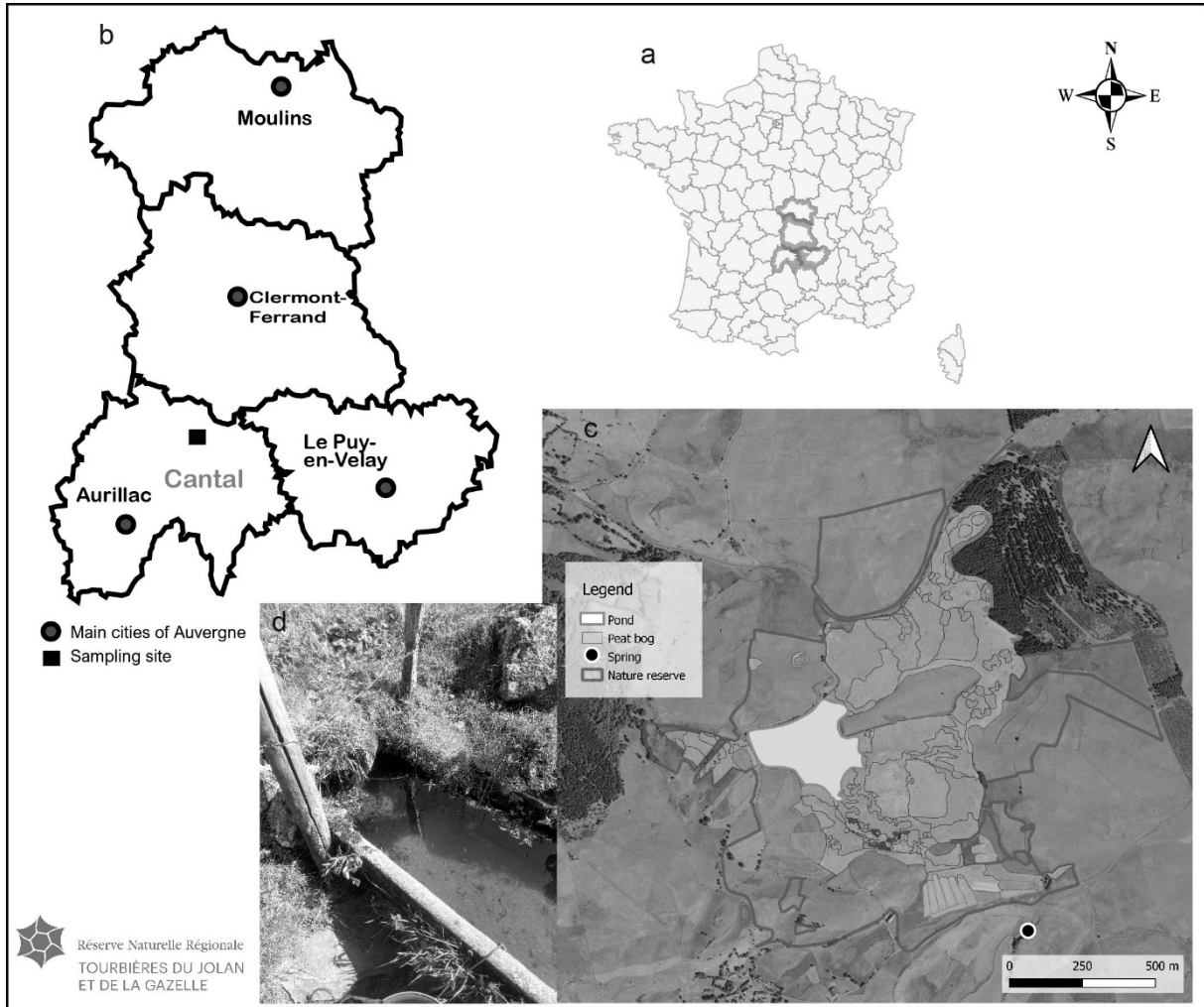
428

429

430

431

432 Figure 1. Map showing the location of the study spring. a and b: general location of the spring
433 in France and in the Auvergne region; c: location of the spring (blue circle) in Regional
434 Nature Reserve (RNR) of the Jolan and Gazelle peatlands; d: photography of the studied
435 spring.

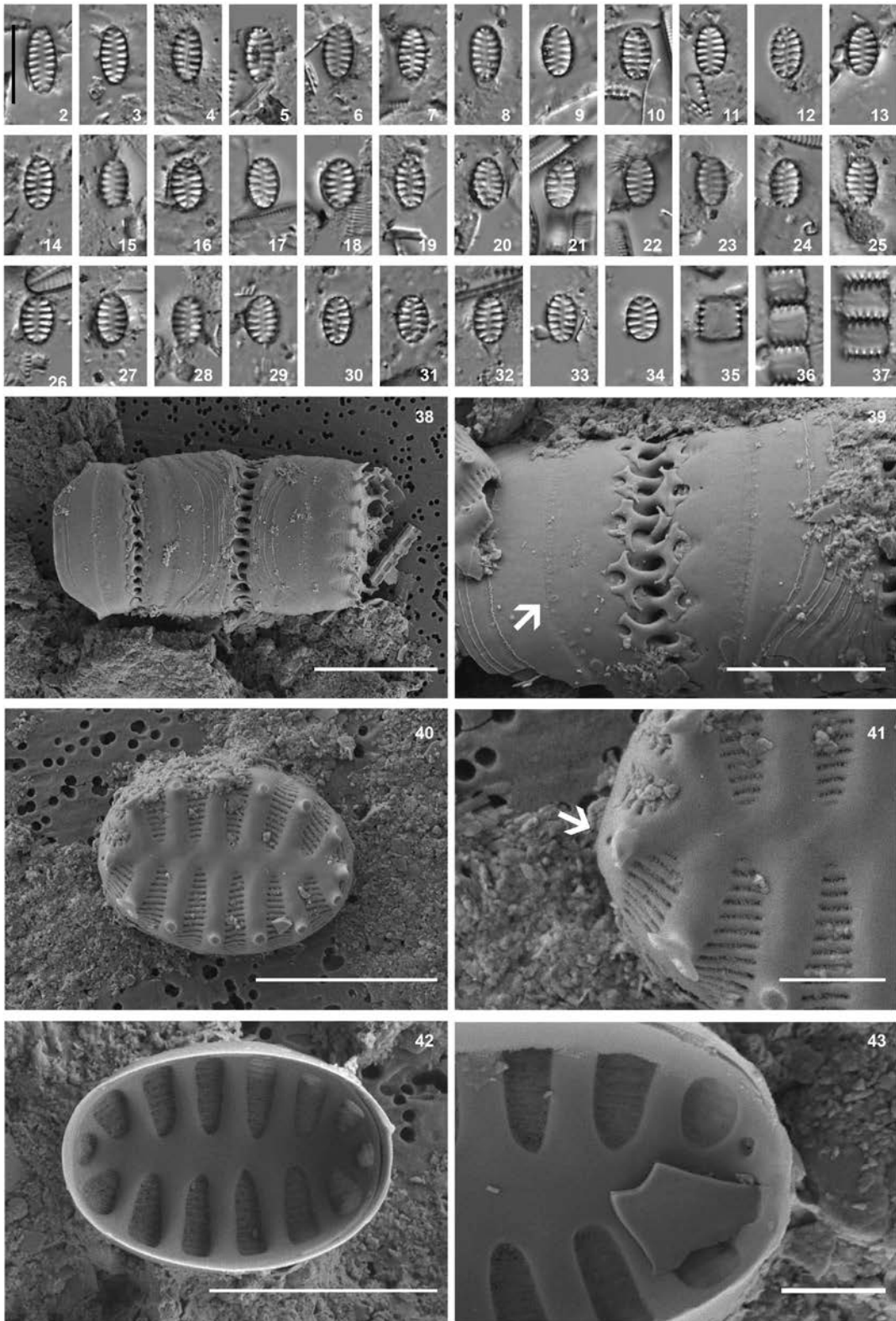


448

449

450 Figures 2–43. *Staurosirella luectoriana* sp. nov. Figs 2–37. LM. Type population of a spring
451 of the RNR of the Jolan and Gazelle peatlands, France. Scale bar = 10 μm . Figs 38–43. SEM.
452 Figs 38. External view of two frustules and one valve connected to each other with
453 dichotomously branched and interlocking spines. Fig. 39. External detail of the linking spines.
454 The arrow indicates the presence of mantle plaques. Fig. 40. External view of an entire valve.
455 Fig. 41. External detail of the apex. The arrow indicates the reduced APF. Fig. 42. Internal
456 view of an entire valve. Fig. 43. Internal detail of the apex. Scale bar = 5 μm (Fig. 38), 4 μm
457 (Figs 40, 42), 3 μm (Fig. 39) and 1 μm (Figs 41, 43).

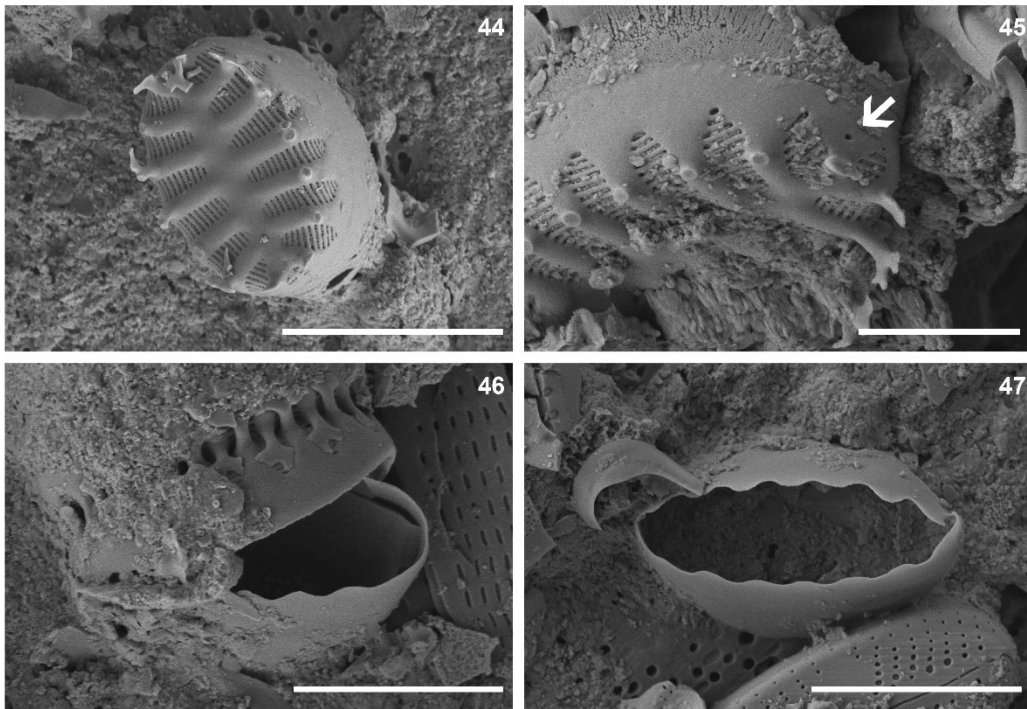
458



459

460

461 Figures 44–47. Fig 44. External view of a tilted valve. Apical pore field replaced by vestiges
462 of a stria, reduced to rounded areolae. Fig. 45. External view of the apex. The arrow indicates
463 the reduced APF composed of only one pore. Figs 46–47. Valvocopula bearing fimbriae.
464 Scale bar = 5 μm (Fig. 44), 4 μm (Figs 46, 47) and 2 μm (Fig. 45).
465



466